Perry, M., Kakar, N., Ischuk, A., Metzger, S., Bendick, R., Molnar, P., Mohadjer, S. (2019): Little Geodetic Evidence for Localized Indian Subduction in the Pamir-Hindu Kush of Central Asia. - *Geophysical Research Letters*, *46*, 1, pp. 109—118.

DOI: http://doi.org/10.1029/2018GL080065

Geophysical Research Letters

RESEARCH LETTER
10.1029/2018GL080065

Key Points:
- Crustal shortening is accommodated across the northern margins of the Pamir and Hindu Kush between NW Afghanistan and the Tajik Depression
- There is little geodetic evidence for localized crustal shortening on the south side of the Hindu Kush between Indian and Pamir crust
- Intermediate depth seismicity in the Hindu Kush cannot easily be linked to ongoing subduction of Indian lithosphere

Supporting Information:
- Supporting Information S1
- Table S1
- Table S2

Correspondence to:
M. Perry,
mason.perry@umontana.edu

Citation:
Perry, M., Kakar, N., Ischuk, A., Metzger, S., Bendick, R., Molnar, P., & Mohadjer, S. (2019). Little geodetic evidence for localized Indian subduction in the Pamir-Hindu Kush of Central Asia. *Geophysical Research Letters*, *46*, 109–118. https://doi.org/10.1029/2018GL080065

Received 20 AUG 2018
Accepted 12 DEC 2018
Accepted article online 17 DEC 2018
Published online 3 JAN 2019

Little Geodetic Evidence for Localized Indian Subduction in the Pamir-Hindu Kush of Central Asia

M. Perry[1], N. Kakar[2], A. Ischuk[3], S. Metzger[4], R. Bendick[1], P. Molnar[5], and S. Mohadjer[6]

[1]Department of Geosciences, University of Montana, Missoula, MT, USA, [2]Norwegian Afghanistan Committee, Kabul, Afghanistan, [3]Institute of Geology, Earthquake Engineering and Seismology, The Academy of Sciences of the Republic of Tajikistan, Dushanbe, Tajikistan, [4]Lithosphere Dynamics, GFZ German Research Centre for Geosciences, Potsdam, Germany, [5]Department of Geological Sciences, University of Colorado Boulder, Boulder, CO, USA, [6]Department of Geosciences, University of Tübingen, Tübingen, Germany

Abstract Geodetically derived velocities from Central Asia show that Northern Afghanistan, the Tajik Pamir, and northwestern Pakistan all move northward with comparable large velocities toward Eurasia. Steep velocity gradients, hence high strain rates, occur only across the Main Pamir Fault zone and with lesser magnitude between the northernmost Hindu Kush and the south and southeast margins of the Tajik Depression. Localized shortening is not apparent on any active India-Hindu Kush crustal boundary; hence, crustal convergence between India and Eurasia in Central Asia is absorbed primarily on the northern and western margins of the Pamir. This concentrated strain on the Pamir margins is consistent with one, geometrically complex, interface between subducting Asian lithosphere and the Pamir. That interface might curve westward such that the Hindu Kush seismic zone is a continuation of the Pamir seismic zone, or alternatively, Hindu Kush earthquakes might occur in convectively unstable mantle lithosphere mechanically detached from surface faults.

Plain Language Summary Using Global Positioning System (GPS) measurements of surface velocities, we find that much of the relative motion between India and Eurasia in Central Asia is accommodated on a single crustal boundary on the north side of the Pamir, wrapping around the eastern and southern margins of the Tajik Depression.

1. Introduction

The Pamir-Hindu Kush region of Central Asia (Figure 1) serves as the best present-day example of ongoing subduction of continental lithosphere. It is interpreted as a case of initiation of subduction in continental materials (Burtman & Molnar, 1993; Hamburger et al., 1992; Jay et al., 2017; Kufner et al., 2016; Negredo et al., 2007; Pegler & Das, 1998; Schneider et al., 2013; Sippl, Schurr, Yuan, et al., 2013), in contrast to the more common scenario where continental lithosphere follows oceanic lithosphere into a subduction zone. Because subduction is generally attributed to gravitational foundering of negatively buoyant intact lithosphere into the asthenosphere (Isacks et al., 1968), while continental lithosphere is usually thought to be less dense than the mantle regardless of age, such subduction is unusual (McKenzie, 1969, 1977; Turcotte et al., 1977).

Beneath the Pamir and the Hindu Kush, a seismogenic zone reaching to approximately 350-km depth (Sippl, Schurr, Yuan, et al., 2013) has several subduction features, including crustal thrust faults (Burtman & Molnar, 1993), localized seismicity (e.g., Pavlis & Hamburger, 1991; Prieto et al., 2012; Sippl, Schurr, Yuan, et al., 2013), and a zone of high seismic wave speeds and low seismic attenuation extending to mantle depths (e.g., Khalturin et al., 1977; Mellors et al., 1995; Schneider et al., 2013; Sippl, Schurr, Tympel, et al., 2013). The distribution of earthquake hypocenters below the crust is conventionally divided into two parts, a northeastern part beneath the Pamir and a southwestern part beneath the Hindu Kush (Figure 1), distinguished by the Pamir zone dipping shallowly to the south and the Hindu Kush zone dipping nearly vertically to the north (Billington et al., 1977; Chatelain et al., 1980; Roecker, 1982; Roecker et al., 1980; Sippl, Schurr, Yuan, et al., 2013), with the two separated by a gap in hypocenters at depth. Fan et al. (1994), Kufner et al.

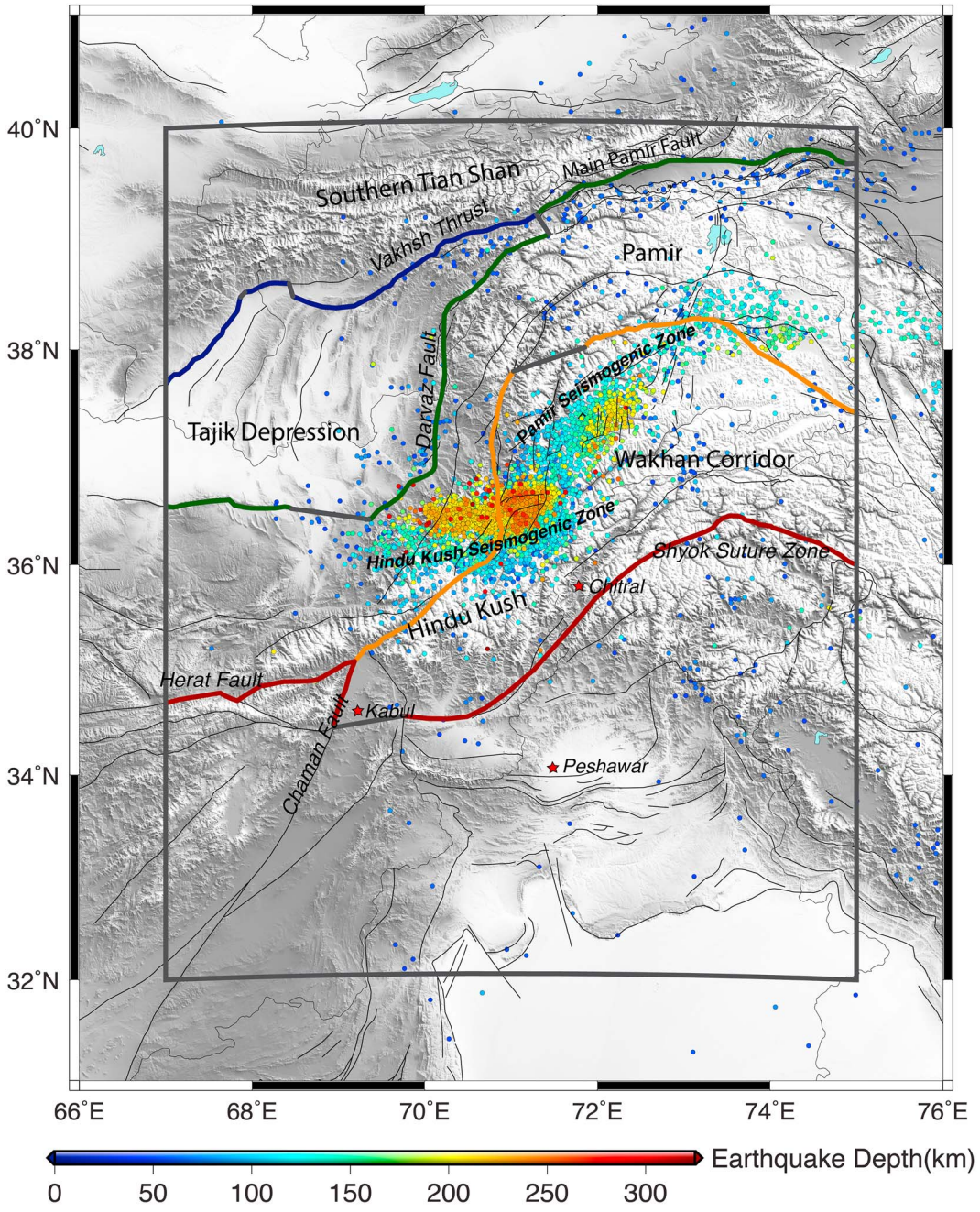

Figure 1. Map of the study area. Earthquakes below 50 km are plotted and colored by depth. Major faults and geographic features are labeled. Thin black lines represent known faults from Mohadjer et al. (2016). Thick colored lines represent the progression of block modeling (Table 1). The single boundary model is represented by the green line; the two-boundary model adds a boundary south of the Hindu Kush shown by the red line. The three- and four-boundary models add further boundaries denoted by the blue and orange lines, respectively. Gray lines represent free slip boundaries on the edges of the model domain and segments of modeled boundaries that do not correspond to mapped structures.

(2016), and Liao et al. (2017), among others, attribute both the reversal in dip direction and the gap in seismicity at depth to different sources of lithosphere for each part of the seismic zone, with the Pamir zone of Eurasian origin and the Hindu Kush zone of Indian origin. This "two-sided" scenario corresponds to the two-boundary models discussed below (model family 2). Because of the absence of a gap in the distribution of seismic hypocenters shallower than 80–100 km (Sippl, Schurr, Yuan, et al., 2013), as well as the narrowness of the deeper gap below ~100-km depth, others interpret Pamir-Hindu Kush

intermediate depth earthquakes as indicative of a single warped slab of lithosphere, of Indian (Pegler & Das, 1998), or Asian origin (Sippl, Schurr, Yuan, et al., 2013). The latter "one-sided" subduction corresponds to the one-boundary models discussed below (model family 1). An alternative model for the one-boundary models allows a downgoing, intact lithospheric slab hosting Pamir seismicity while Hindu Kush seismicity occurs in a negatively buoyant blob of mantle lithosphere, analogous to the interpretation that Houseman and Gemmer (2007) and Lorinczi and Houseman (2009) gave for the Vrancea zone beneath the Carpathians.

On the northern margin of the Pamir (Figure 1), geodetic (Ischuk et al., 2013; Metzger et al., 2018; Reigber et al., 2001; Zubovich et al., 2010) and geologic (Arrowsmith & Strecker, 1999; Burtman & Molnar, 1993; Cowgill, 2010; Li et al., 2012; Nikonov et al., 1983; Strecker et al., 1995; Trifonov, 1978, 1983) observations are consistent with mechanical continuity of subducted and surface lithosphere with a discrete interface between overriding and downgoing crust manifested as localized and persistent shortening at the Main Pamir Fault system. Schneider et al. (2013) show receiver functions interpreted as the top and bottom of Asian crust that has been subducted southward beneath the overriding Pamir. Several other studies find high-speed zones surrounding the intermediate depth earthquakes and extending deeper (e.g., Koulakov & Sobolev, 2006; Kufner et al., 2016; Mellors et al., 1995; Mohan & Rai, 1995; Vinnik & Lukk, 1973, 1974). Furthermore, northward deflections of geologic units within the Pamir relative to their continuations in Afghanistan and Tibet (Burtman & Molnar, 1993; Cowgill, 2010; Sobel et al., 2013) suggest 300 km of northward displacement past the Tajik Depression and Tarim Basin. Finally, the 2015 Murghab earthquake (Metzger et al., 2017; Sangha et al., 2017) demonstrates ongoing thrusting of the Pamir northward over the Alai Valley; two moderate events in 1972 and 1982 show thrusting of the Hindu Kush westward over the Tajik Depression (Abers et al., 1988), while crustal earthquakes within the Pamir show predominantly normal and strike-slip faulting with east-west extension (Strecker et al., 1995).

In contrast to the Pamir, although the high seismic velocity anomaly beneath the Hindu Kush (Figure 1) is spatially coincident with hypocenters (Koulakov & Sobolev, 2006; Kufner et al., 2016; Mohan & Rai, 1995; Negredo et al., 2007), it does not project to a unique thrust fault at the surface (Sippl, Schurr, Tympel, et al., 2013). Moreover, strain rates inferred from seismic moments at intermediate depth are much higher than average horizontal convergence rates at the surface (Kufner et al., 2017; Zhan & Kanamori, 2016).

2. Data and Methods

We compile data collected from 2008 to 2016 from 66 Geodetic Positioning System (GPS) stations throughout Tajikistan, Afghanistan, Kyrgyzstan, and Pakistan, including 32 publicly available and 9 restricted campaign sites and 25 regional continuous sites including International GNSS Service (IGS) reference stations (Table S1 in the supporting information). We process these data using the GAMIT/GLOBK software package (Herring et al., 2015) following the procedure described in Reilinger et al. (2006). GAMIT is used to calculate initial daily position estimates of each station. These are edited, averaged, and weighted over approximately 2-week long intervals. GLOBK's Kalman filter is used to estimate linear horizontal velocities from the position averages, incorporating a random walk noise model to account for systematic errors. The velocity solution is tied to the International Terrestrial Reference Frame 2008 (ITRF08) and then transformed into a stable Eurasian reference frame using the ITRF08-Eurasia angular velocity calculated by Altamimi et al. (2012; Table S1).

Following the determination of the regional velocities, we define five families of models (0, 1, 2, 3, and 4) based on the number of tectonic boundaries in the study area (Figures S1–S4). We use TDEFNODE (McCaffrey, 2009) to calculate angular velocities for rigid crustal domains that minimize misfit to the observed velocity field. We use the misfit calculated in TDEFNODE as a measure of the likelihood function of possible tectonic boundaries on the north margin of the Pamir; the north, east, and south margins of the Tajik Depression; within the central Pamir; and south of the Hindu Kush (Figure 1). Because we only use the TDEFNODE results for misfit related to the presence or absence of particular tectonic boundaries, the resulting block models do not necessarily describe the full regional kinematics.

We set the specific location of boundaries using major faults in the Central Asia Fault Database (Mohadjer et al., 2016). Lacking detailed 3-D structural information about these faults, we approximate them as 20° dipping fault planes for thrust faults, 45° dipping planes for normal faults, and near-vertical fault planes for strike-slip faults. The TDEFNODE inversions are not sensitive to the structural geometry (such as 3-D fault shape, dip angle, or locking depth) because very few of the observed geodetic velocities are located within the

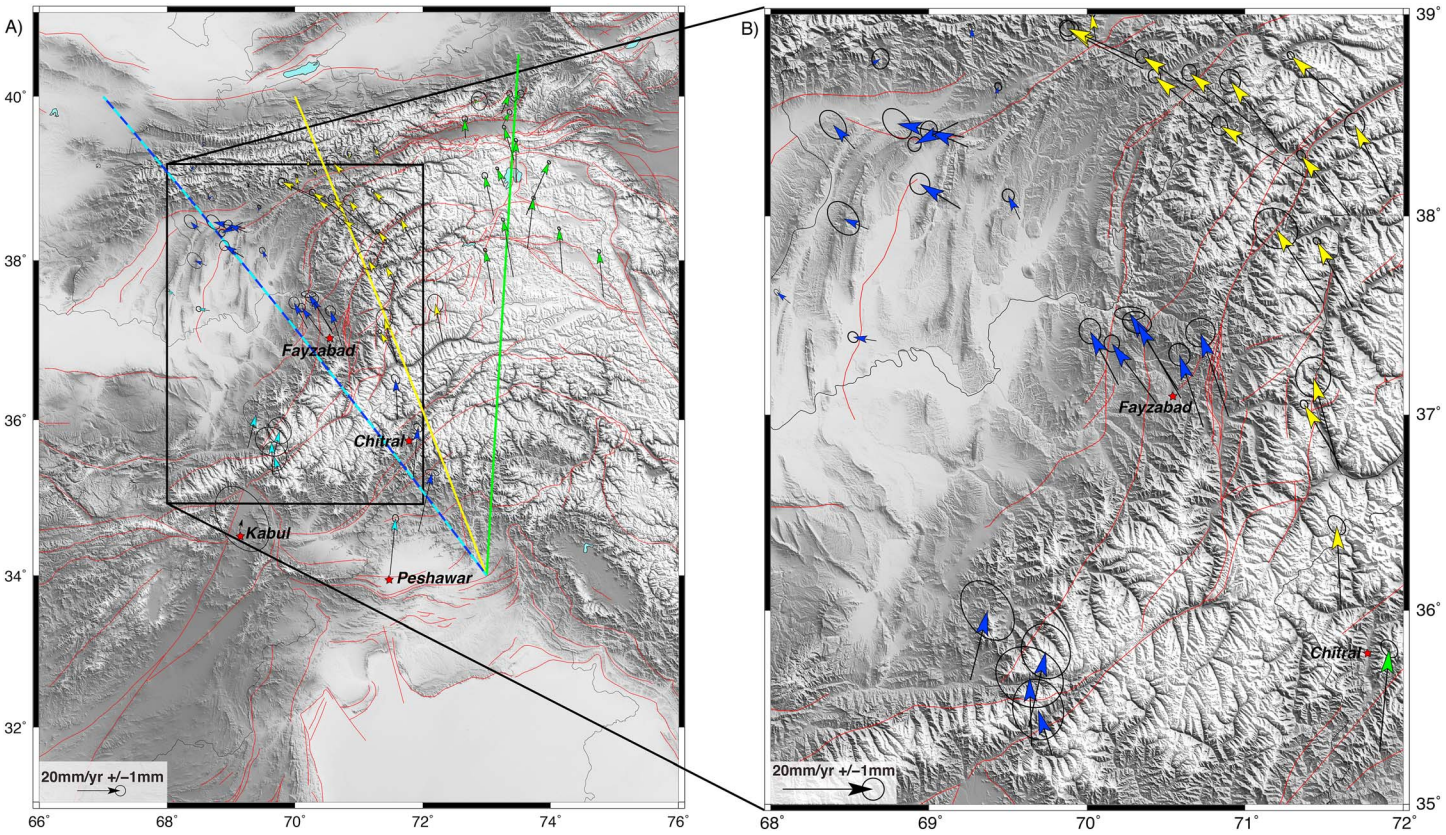

Figure 2. Velocity solution in a Eurasia-fixed frame with 95% confidence ellipses and regional faults from Mohadjer et al. (2016) in red. (a) Overview of velocity solution with colored lines corresponding to velocity profiles (Figure 3). (b) Zoomed in map showing velocity observations in Northern Afghanistan. The locations of profiles in Figure 3 are shown as colored lines.

elastic length scale of the block bounding faults. The zero-boundary case (model 0) corresponds to a rigid rotation of the whole study area, the one-boundary case (model 1a or 1b, Figure S1) to convergence between Eurasia and India on the Main Pamir Fault and its westward extension along the Darvaz-Karakul' Fault, the two-boundary case (model 2b, Figure S2) to convergence between Eurasia and the Pamir at the Main Pamir Fault and between the Pamir-Hindu Kush and India on a structure south of the Hindu Kush, and the three- and four-boundary approximations to additional active boundaries on the north side of the Tajik Depression and within the central Pamir, respectively (Figure 1). We present alternative configurations for each number of boundaries in the supporting information (Table S2 and Figures S1–S4). Boundaries defining the far-field edges of the model domain are specified for geometric simplicity rather than geologic or kinematic accuracy (Figure 1 and Figures S1–S4).

We then compare model favorability using the Akaike Information Criterion (AIC) and a modified version for limited observational data (AICc; Akaike, 1974). These tools are designed for model selection in nonunique problems by penalizing both large misfits to data and large numbers of free parameters. We specifically use the least squares case of the AIC and the AICc, $\mathrm{AIC} = n\log\left(\widehat{\sigma}^2\right) + 2K$ and $\mathrm{AIC_c} = \mathrm{AIC} + \frac{2K(K+1)}{n-K-1}$, respectively (Burnham & Anderson, 2002), where n is the number of GPS velocity observations, $\widehat{\sigma}^2$ is the root-mean-square misfit determined from the TDEFNODE inversion, and K is the number of free parameters. K increases by 4 with each additional boundary in the kinematic model, because the existence of the boundary and three parameters defining the angular velocity of the resulting additional block are added.

3. Kinematic Results

The GPS velocities (Figures 2 and 3 and Table S1) show ongoing convergence between India and Eurasia, with the steepest velocity gradients localized near the northern margin of the Pamir, consistent with other

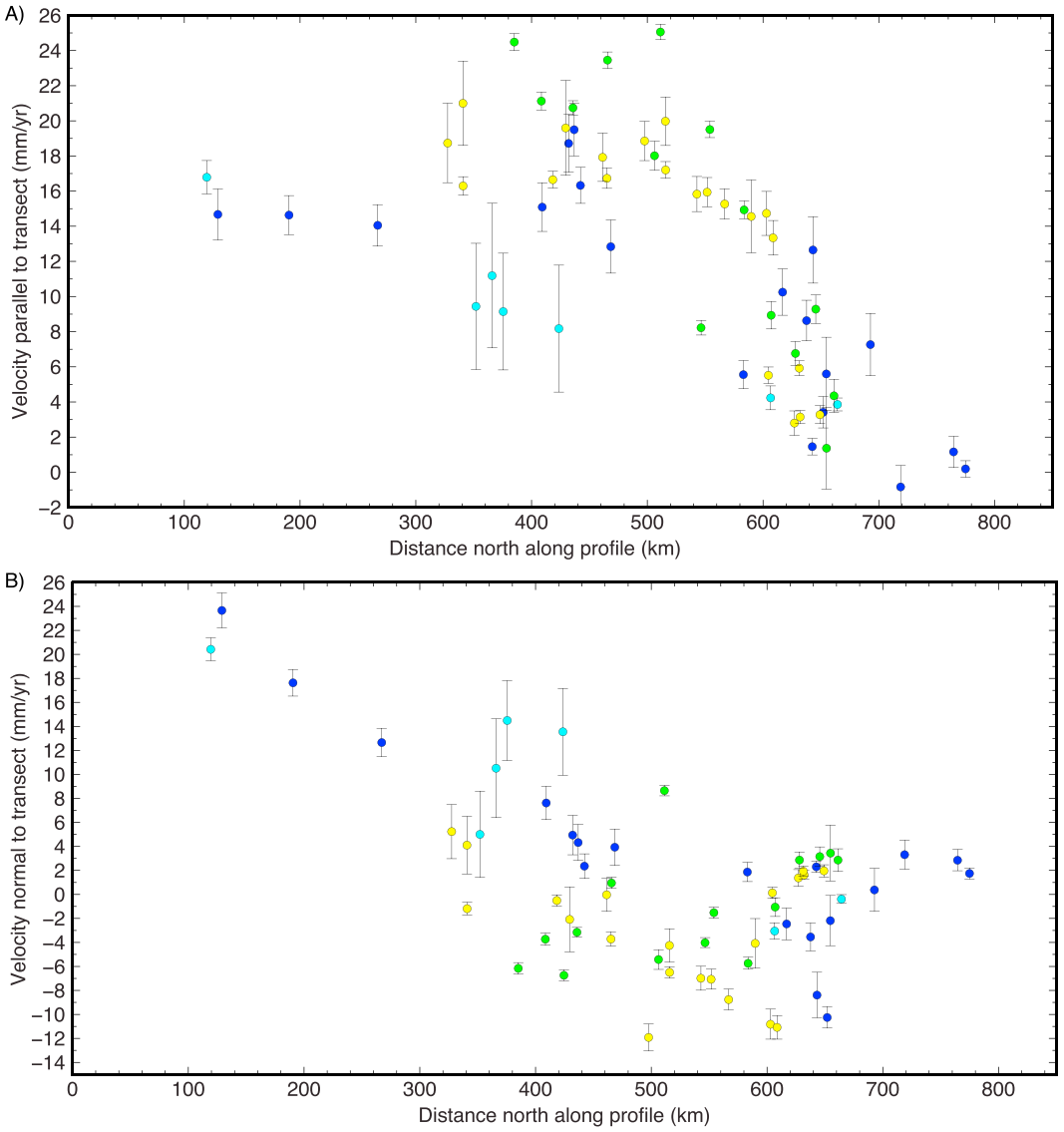

Figure 3. Eurasia-fixed velocities decomposed into (a) profile-parallel (shortening) and (b) normal (shear) components. Station color corresponds to colored profiles shown in Figure 2.

GPS results (Ischuk et al., 2013; Reigber et al., 2001; Zhou et al., 2016; Zubovich et al., 2010). The shortening rate on and adjacent to the Main Pamir Fault system is 18–22 mm/year (65–80% of the total India-Eurasia relative rate of 28 ± 4 mm/year, measured from Karachi; Mohadjer et al., 2010), increasing along strike eastward (Figures 2 and 3). Convergence across the Alai Valley, the topographic margin of the Pamir, accommodates ~15 mm/year of this total N-S convergence across less than 50 km centered on or near the Main Pamir Fault (e.g., Burtman & Molnar, 1993; Ischuk et al., 2013; Liao et al., 2017; Zubovich et al., 2016) and Vakhsh Thrust. Between the Western Pamir and the Tajik Depression, there is approximately 15 mm/year of NW-SE convergence (Figure 3). Sites in the western Tajik Depression move with negligible velocities relative to Eurasia (Figures 2 and 3).

The southern margin of the Pamir-Hindu Kush-Karakorum from Peshawar to Chitral accommodates not more than 10 mm/year of India-Asia convergence over >250 km (Figures 2 and 3). Little convergence is allowed south of Peshawar, such as on the Salt Range Front Fault, since Karachi (KCHI in Table S1) moves north toward stable Eurasia at about 28 mm/year, while Peshawar (NCEG in Table S1) moves north at about 26 mm/year (Ischuk et al., 2013; Mohadjer et al., 2010). The Central and Northern Pamir also move only slightly less rapidly than Peshawar, at 18–24 mm/year relative to Eurasia

Table 1
Table Summarizing AIC Model Selection

Model	Boundaries	K	n	RMS	AIC	ΔAIC	AICc	ΔAICc	Notes
0	0	4	63	9.80	295.59	39.10	296.28	37.12	No boundary
1a	1	8	63	6.74	256.49	0.00	259.15	0.00	Figure 1 green boundary
2c	2	12	63	6.60	261.79	5.30	268.03	8.88	Figure 1 green + red boundaries
3b	3	16	63	6.38	265.53	9.04	277.36	18.20	Figure 1 green + red + blue
4	4	20	63	6.36	273.14	16.65	293.14	33.98	Figure 1 green + red + blue + orange

Note. The lowest calculated AICc and ΔAICc values of zero represent the most favorable model of those tested. AIC = Akaike Information Criterion; RMS = root-mean-square.

(Ischuk et al., 2013), precluding rapid north-south shortening in the Wakhan Corridor or southernmost Tajikistan (Figures 2 and 3).

GPS installations around Fayzabad, Afghanistan, between the High Hindu Kush and the Darvaz-Karakul' Fault converge at about 18 mm/year with Eurasia, like those in the western Pamir (Figure 2b). This includes at most 10 mm/year of shortening between the Hindu Kush and the Tajik Depression perpendicular to the eastern margin of the Depression. Velocities at sites further to the southwest, just north of Kabul, are slightly slower, converging with Eurasia at 10–12 mm/year (Figure 3) and with the Tajik Depression at 6–8 mm/year. The Fayzabad sites move nearly perpendicular to the trend of the Hindu Kush with SW-NE shear components of 1–2 mm/year. Sites closer to Kabul have somewhat larger shear components of 4–8 mm/year.

4. Model Selection Results

The ΔAICc (Tables 1 and S2) compares the favorability of plausible tested models. The smallest AICc score corresponds to the model with the most empirical support; small ΔAICc values indicate models of similar favorability. Larger ΔAICc values indicate either that total misfit is large, that there are many underconstrained free parameters, or both.

Unsurprisingly, based on the AICc scores, a rigid rotation model with no boundaries is the least favorable, with the maximum ΔAICc of the configurations tested. Adding a curving boundary at the location of the steepest velocity gradients (green line in Figure 1) minimizes the AIC and AICc (Tables 1 and S2), indicating the most favored (in the AIC sense) model among those that describe the deformation in terms of boundaries. An alternative boundary on the north side of the Tajik Depression gives a similar AICc (ΔAICc = 1.7; Table S2), indicating that the observations support either variant, and we cannot distinguish between a boundary on the north or south side of the Tajik Depression with the available observations. However, a model with boundaries on both sides of the Tajik Depression is less favorable (Figures S1–S4 and Table S2). Adding an additional boundary on the south side of the Hindu Kush increases the AIC and AICc by 5.3 and 8.9, respectively, for a model that is considerably less favorable but still with some empirical support (Tables 1 and S2). Adding additional boundaries through the Central Pamir produces unfavorable models, with large ΔAICc. Therefore, the presence of Eurasian lithosphere underthrusting the Main Pamir Fault footwall is well constrained by the velocity observations, but a slab of Indian lithosphere attached to the surface and underthrusting the Hindu Kush either south of or within the zone of anomalous seismicity is less so.

5. Discussion

Three explanations have been proposed for the Pamir-Hindu Kush intermediate depth earthquake zone: a contorted subducting slab of Eurasian material (one-sided subduction; Figure 4a), distinct slabs of Eurasian and Indian origin subducting beneath the Pamir and Hindu Kush, respectively (two-sided subduction; Figure 4b; e.g., Burtman & Molnar, 1993; Kufner et al., 2017; Liao et al., 2017), and foundering lithosphere (one-sided subduction plus convective overturn; Fillerup et al., 2010; Houseman & Gemmer, 2007; Lorinczi & Houseman, 2009). The first of these options is consistent with available constraints from prior geodesy (Ischuk et al., 2013; Mohadjer et al., 2010; Zhou et al., 2016; Zubovich et al., 2010) and the additional results presented here, plus slip on known faults (Arrowsmith & Strecker, 1999; Bernard et al., 2000; Coutand et al., 2002; Cowgill, 2010; Kuchai & Trifonov, 1977; Nikonov et al., 1983; Sobel et al., 2011; Strecker et al., 1995; Trifonov, 1978, 1983) and seismic imaging (e.g., Schneider et al., 2013; Sippl, Schurr,

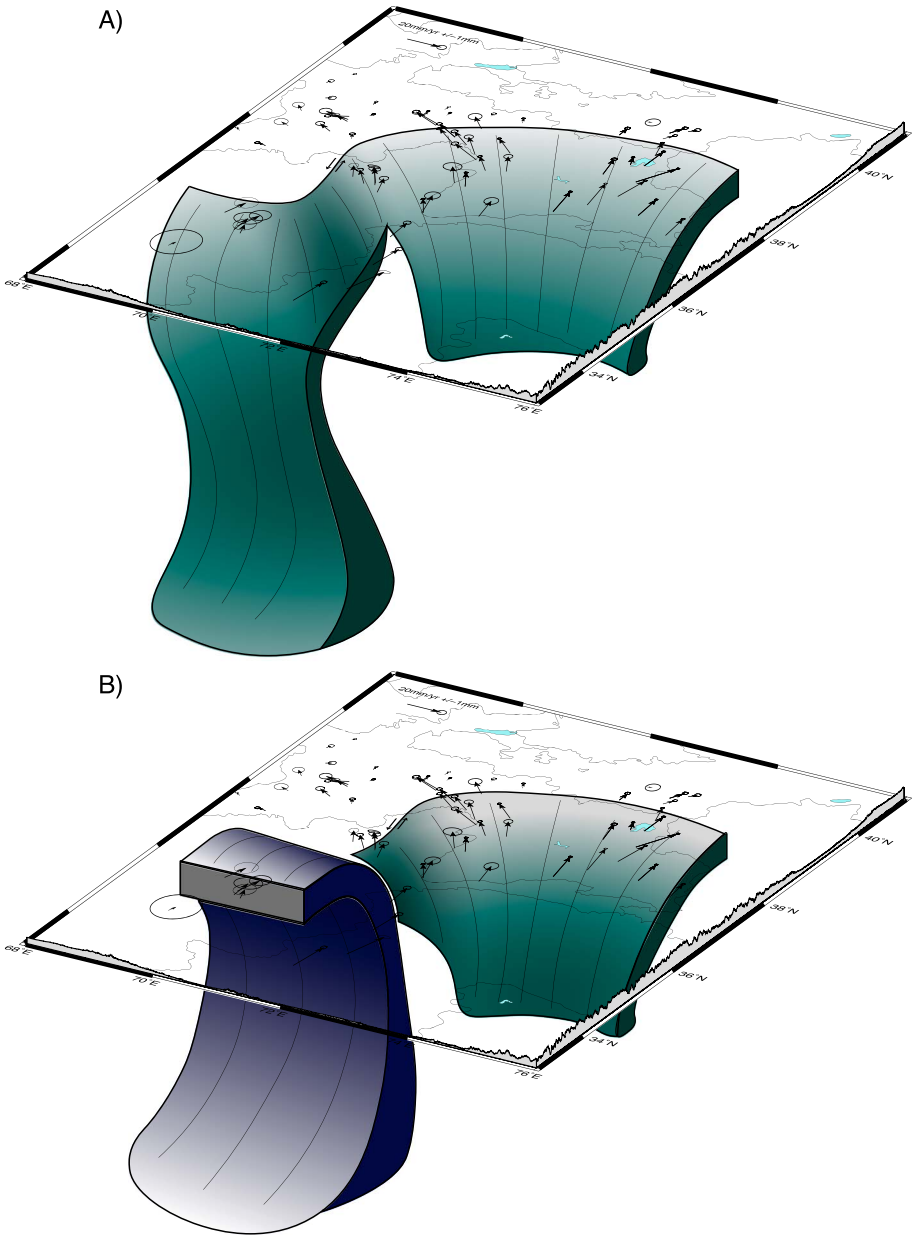

Figure 4. Cartoons showing two endmember models. (a) One of the possible "one-sided" models (model family 1) with a convoluted geometry of downgoing Eurasian lithosphere. Note that whether the surface intersection of the contorted slab wraps around the northern or southern side of the Tajik Depression is not distinguished by the AICc results. Furthermore, surface velocities from geodesy cannot constrain the arrangement of lithosphere at depth, only whether it is attached to the surface or not. Therefore, the one-sided endmember allows Hindu Kush intermediate depth seismicity to be hosted in either the deepest part of a Eurasian slab as depicted, in a detached Indian slab, or in a foundering "blob" of Hindu Kush-Pamir lithosphere. (b) "Two-sided" model (model family 2) with downgoing Eurasian and Indian lithosphere, the former hosting intermediate depth Pamir seismicity and the latter hosting intermediate depth Hindu Kush seismicity.

Tympel, et al., 2013), except for the inferred rapid sinking of the deepest part of the Hindu Kush anomaly from moment summation (Kufner et al., 2017; Zhan & Kanamori, 2016). Such a single slab model implies relatively simple dynamics: subduction needs to initiate and persist only once in continental lithosphere, presumably in an area of previous crustal thinning (Leith, 1982). In the single-slab case ~15–35% of the total India-Eurasia rate is accommodated south of the Pamir throughout the broadly distributed region of high topography. Alternatively, if Indian lithosphere hosts Hindu Kush intermediate depth seismicity, the

Indian material must be mostly or entirely detached from the surface, such that there is no longer an active, high strain rate thrust system separating downgoing Indian lithosphere from overriding Hindu Kush crust. A third option, convective instability arising from lithospheric thickening, has been invoked in the Carpathians (Houseman & Gemmer, 2007; Lorinczi & Houseman, 2009; Fillerup et al., 2010) and also matches the observed lack of a surface boundary as well as the spatial distribution of intermediate depth seismicity and inferred high stretching rates (Kufner et al., 2017; Zhan & Kanamori, 2016). In this case, the origin of the foundering material could be Indian, Eurasian, or Tethyan lithosphere.

Although subduction is generally thought to initiate in old oceanic lithosphere (e.g., Carlson et al., 1983; McKenzie, 1977; Turcotte et al., 1977; Stein & Stein, 1996), which is typically more dense than asthenosphere, subduction of Eurasian continental lithosphere at the Pamir is now supported by many different observations and demonstrates at least the possibility of subduction initiation within continental lithosphere (Burtman & Molnar, 1993; Chatelain et al., 1980; Jay et al., 2017). Combined with the possibility of a Hindu Kush example of convective overturn of continental lithosphere like that invoked in the Carpathians (Houseman & Gemmer, 2007; Fillerup et al., 2010; Lorinczi & Houseman, 2009) or detachment of an Indian lithospheric slab, we infer greater exchange of mass between the continental lithosphere and the asthenosphere than has previously been assumed likely.

6. Conclusion

Most of the convergence between India and Eurasia is accommodated on the northern side of the Pamir and between the Fayzabad-area (NE Afghanistan) and the Tajik Depression. Based on an AIC, the most favorable regional tectonic boundary model of the options considered consists of a single tectonic boundary extending from the Main Pamir Fault to thrusts wrapping around the eastern and southern margins of the Tajik Depression then linking to the Chaman Fault system through Afghanistan (Lawrence et al., 1992; Szeliga et al., 2012). Additional tectonic boundaries introduce more free parameters to models without fitting the surface velocities much better. The paucity of localized shortening south of the Hindu Kush therefore favors one-sided subduction at the Pamir, at least in the present day, rather than two-sided subduction invoked in several recent dynamic models (e.g., Kufner et al., 2017; Liao et al., 2017; Schurr et al., 2014). One-sided models allow Hindu Kush seismicity to be hosted in the overturned Asian slab, a detached Indian slab, or convectively foundering lithosphere. Shortening in the Pamir-Hindu Kush-Karakorum is much slower and much more diffuse than at the Main Pamir Fault, precluding a present-day India-Hindu Kush subduction boundary in the crust.

Acknowledgments
This research was supported by the Crafoord Foundation, GFZ, and the University of Montana. Major logistical support was provided by the Tajik Institute of Earthquake Engineering and Seismology and the Norwegian Afghanistan Commission. All plots and maps were made using GMT mapping tools (Wessel et al., 2013). The velocity solution is available at https://doi.org/10.5281/zenodo.1469091.

References

Abers, G., Bryan, C., Roecker, S., & McCaffrey, R. (1988). Thrusting of the Hindu Kush over the southeastern Tadjik Basin, Afghanistan: Evidence from two large earthquakes. *Tectonics*, *7*(1), 41–56. https://doi.org/10.1029/TC007i001p00041

Akaike, H. (1974). A new look at the statistical model identification. *IEEE Transactions on Automatic Control*, *19*(6), 716–723. https://doi.org/10.1109/TAC.1974.1100705

Altamimi, Z., Métivier, L., & Collilieux, X. (2012). ITRF2008 plate motion model. *Journal of Geophysical Research*, *117*, B07402. https://doi.org/10.1029/2011JB008930

Arrowsmith, J. R., & Strecker, M. R. (1999). Seismotectonic range-front segmentation and mountain-belt growth in the Pamir-Alai region, Kyrgyzstan (India-Eurasia collision zone). *Bulletin of the Geological Society of America*, *111*(11), 1665–1683. https://doi.org/10.1130/0016-7606(1999)111<1665:SRFSAM>2.3.CO;2

Bernard, M., Shen-Tu, B., Holt, W. E., & Davis, D. M. (2000). Kinematics of active deformation in the Sulaiman Lobe and Range, Pakistan. *Journal of Geophysical Research*, *105*(B6), 13,253–13,279. https://doi.org/10.1029/1999JB900405

Billington, S., Isacks, B. L., & Barazangi, M. (1977). Spatial distribution and focal mechanisms of mantle earthquakes in the Hindu Kush–Pamir region: A contorted Benioff zone. *Geology*, *5*(11), 699–704. https://doi.org/10.1130/0091-7613(1977)5<699:SDAFMO>2.0.CO;2

Burnham, K. P., & Anderson, D. R. (2002). *Model selection and multimodel inference: A practical information-theoretic approach* (2nd ed.). New York: Springer. https://doi.org/10.1016/j.ecolmodel.2003.11.004

Burtman, V. S., & Molnar, P. H. (1993). Geological and geophysical evidence for deep subduction of continental crust beneath the Pamir. *Geological Society of America Special Papers*, *281*, 76.

Carlson, R. L., Hilde, T. W., & Uyeda, S. (1983). The driving mechanisms of plate tectonics: Relation to age of lithosphere at trenches. *Geophysical Research Letters*, *10*(4), 297–300. https://doi.org/10.1029/GL010i004p00297

Chatelain, J. L., Roecker, S. W., Hatzfeld, D., & Molnar, P. (1980). Microearthquake seismicity and fault plane solutions in the Hindu Kush region and their tectonic implications. *Journal of Geophysical Research*, *85*(B3), 1365–1387. https://doi.org/10.1029/JB085iB03p01365

Coutand, I., Strecker, M. R., Arrowsmith, J. R., Hilley, G., Thiede, R. C., Korjenkov, A., & Omuraliev, M. (2002). Late Cenozoic tectonic development of the intramontane Alai Valley, (Pamir-Tien Shan region, central Asia): An example of intracontinental deformation due to the Indo-Eurasia collision. *Tectonics*, *21*(6), 1053. https://doi.org/10.1029/2002TC001358

Cowgill, E. (2010). Cenozoic right-slip faulting along the eastern margin of the Pamir salient, northwestern China. *Bulletin of the Geological Society of America*, *122*(1–2), 145–161. https://doi.org/10.1130/B26520.1

Fan, G., Ni, J. F., & Wallace, T. C. (1994). Active tectonics of the Pamirs and Karakoram. *Journal of Geophysical Research*, *99*(B4), 7131–7160. https://doi.org/10.1029/93JB02970

Fillerup, M. A., Knapp, J. H., Knapp, C. C., & Raileanu, V. (2010). Mantle earthquakes in the absence of subduction? Continental delamination in the Romanian Carpathians. *Lithosphere*, *2*(5), 333–340. https://doi.org/10.1130/L102.1

Hamburger, M. W., Sarewitz, D. R., Pavlis, T. L., & Popandopulo, G. A. (1992). Structural and seismic evidence for intracontinental subduction in the Peter the First Range, central Asia. *Geological Society of America Bulletin*, *104*(4), 397–408. https://doi.org/10.1130/0016-7606(1992)104<0397:SASEFI>2.3.CO;2

Herring, T. A., King, R. W., Floyd, M. A., & Mcclusky, S. C., (2015). GAMIT/GLOBK reference manual release 10.6. Department of Earth, Atmospheric, and Planetary Sciences, Massachusetts Institute of Technology.

Houseman, G. A., & Gemmer, L. (2007). Intra-orogenic extension driven by gravitational instability: Carpathian-Pannonian orogeny. *Geology*, *35*(12), 1135–1138. https://doi.org/10.1130/G23993A.1

Isacks, B., Oliver, J., & Sykes, L. R. (1968). Seismology and the new global tectonics. *Journal of Geophysical Research*, *73*(18), 5855–5899. https://doi.org/10.1029/JB073i018p05855

Ischuk, A., Bendick, R., Rybin, A., Molnar, P., Khan, S. F., Kuzikov, S., et al. (2013). Kinematics of the Pamir and Hindu Kush regions from GPS geodesy. *Journal of Geophysical Research: Solid Earth*, *118*, 2408–2416. https://doi.org/10.1002/jgrb.50185

Jay, C. N., Flesch, L. M., & Bendick, R. O. (2017). Kinematics and dynamics of the Pamir, Central Asia: Quantifying surface deformation and force balance in an intracontinental subduction zone. *Journal of Geophysical Research: Solid Earth*, *122*, 4741–4762. https://doi.org/10.1002/2017JB014177

Khalturin, V. I., Rautian, T. G., & Molnar, P. (1977). The spectral content of Pamir-Hindu Kush intermediate depth earthquakes: Evidence for a high-Q zone in the upper mantle. *Journal of Geophysical Research*, *82*(20), 2931–2943. https://doi.org/10.1029/JB082i020p02931

Koulakov, I., & Sobolev, S. V. (2006). A tomographic image of Indian lithosphere break-off beneath the Pamir-Hindukush region. *Geophysical Journal International*, *164*(2), 425–440. https://doi.org/10.1111/j.1365-246X.2005.02841.x

Kuchai, V. K., & Trifonov, V. G. (1977). A young left-lateral displacement in the Darvaz-Karakul Fault Zone. *Geotectonics*, *11*, 218–226.

Kufner, S., Schurr, B., Haberland, C., Zhang, Y., Saul, J., Ischuk, A., & Oimahmadov, I. (2017). Zooming into the Hindu Kush slab break-off: A rare glimpse on the terminal stage of subduction. *Earth and Planetary Science Letters*, *461*, 127–140. https://doi.org/10.1016/j.epsl.2016.12.043

Kufner, S. K., Schurr, B., Sippl, C., Yuan, X., Ratschbacher, L., Akbar, A. M., et al. (2016). Deep India meets deep Asia: Lithospheric indentation, delamination and break-off under Pamir and Hindu Kush (Central Asia). *Earth and Planetary Science Letters*, *435*(February), 171–184. https://doi.org/10.1016/j.epsl.2015.11.046

Lawrence, R. D., Khan, S. H., & Nakata, T. (1992). Chaman fault, Pakistan-Afghanistan. *Annales Tectonicae*, *6*, 196–223.

Leith, W. (1982). Rock assemblages in central Asia and the evolution of the southern Asian margin. *Tectonics*, *1*(3), 303–318. https://doi.org/10.1029/TC001i003p00303

Li, T., Chen, J., Thompson, J. A., Burbank, D. W., & Xiao, W. (2012). Equivalency of geologic and geodetic rates in contractional orogens: New insights from the Pamir Frontal Thrust. *Geophysical Research Letters*, *39*, L15305. https://doi.org/10.1029/2012GL051782

Liao, J., Gerya, T., Thielmann, M., Webb, A. A. G., Kufner, S.-K., & Yin, A. (2017). 3D geodynamic models for the development of opposing continental subduction zones: The Hindu Kush–Pamir example. *Earth and Planetary Science Letters*, *480*, 133–146. https://doi.org/10.1016/j.epsl.2017.10.005

Lorinczi, P., & Houseman, G. A. (2009). Lithospheric gravitational instability beneath the Southeast Carpathians. *Tectonophysics*, *474*(1–2), 322–336. https://doi.org/10.1016/j.tecto.2008.05.024

McCaffrey, R. (2009). Time-dependent inversion of three-component continuous GPS for steady and transient sources in northern Cascadia. *Geophysical Research Letters*, *36*, L07304. https://doi.org/10.1029/2008GL036784

McKenzie, D. (1977). The initiation of trenches: A finite amplitude instability. In M. Talwani, W. C. Pitman, & W. M. Ewing (Eds.), *Island arcs, deep sea trenches, and back-arc basins* (Vol. 1, pp. 57–61). Washington, DC: American Geophysical Union. https://doi.org/10.1029/ME001p0057

McKenzie, D. P. (1969). Speculations on the consequences and causes of plate motions. *Geophysical Journal of the Royal Astronomical Society*, *18*(1), 1–32, https://doi.org/10.1111/j.1365-246X.1969.tb00259.x.

Mellors, R., Lukk, A. A., Pavlis, G. L., Hamburger, M. W., & Al-Shukri, H. J. (1995). Evidence for a high-velocity slab associated with the Pamir-Hindu Kush seismic zone. *Journal of Geophysical Research*, *100*(B3), 4067–4078. https://doi.org/10.1029/94JB02642

Metzger, S., Ischuk, A., Zubovich, A., Deng, Z., Schöne, T., Schurr, B., et al. (2018). Observations from four high-resolution GPS profiles across the active margin of the Pamir, Central Asia: Can we discriminate interseismic fault slip-rates, slip partitioning, and even co-seismically triggered slip?. EGU General Assembly, Vol. 20, EGU2018–16410-1.

Metzger, S., Schurr, B., Ratschbacher, L., Sudhaus, H., Kufner, S. K., Schöne, T., et al. (2017). The 2015 Mw7.2 Sarez strike-slip earthquake in the Pamir interior: Response to the underthrusting of India's western promontory. *Tectonics*, *36*, 2407–2421. https://doi.org/10.1002/2017TC004581

Mohadjer, S., Alan Ehlers, T., Bendick, R., Stübner, K., & Strube, T. (2016). A Quaternary fault database for central Asia. *Natural Hazards and Earth System Sciences*, *16*(2), 529–542. https://doi.org/10.5194/nhess-16-529-2016

Mohadjer, S., Bendick, R., Ischuk, A., Kuzikov, S., Kostuk, A., Saydullaev, U., et al. (2010). Partitioning of India-Eurasia convergence in the Pamir-Hindu Kush from GPS measurements. *Geophysical Research Letters*, *37*, L04305. https://doi.org/10.1029/2009GL041737

Mohan, G., & Rai, S. S. (1995). Large-scale three-dimensional seismic tomography of the Zagros and Pamir-Hindukush regions. *Tectonophysics*, *242*(3–4), 255–265. https://doi.org/10.1016/0040-1951(94)00201-J

Negredo, A. M., Replumaz, A., Villaseñor, A., & Guillot, S. (2007). Modeling the evolution of continental subduction processes in the Pamir-Hindu Kush region. *Earth and Planetary Science Letters*, *259*(1–2), 212–225. https://doi.org/10.1016/j.epsl.2007.04.043

Nikonov, A. A., Vakov, A. V., & Veselov, I. A. (1983). *Seismotectonics and earthquake zones near the Pamir and Tien Shan* [in Russian] (240 pp.). Nauka, Moscow.

Pavlis, G., & Hamburger, M. (1991). Aftershock sequences of intermediate-depth earthquakes in the Pamir-Hindu Kush seismic zone. *Journal of Geophysical Research*, *96*(B11), 18,107–18,117. https://doi.org/10.1029/91JB01510

Pegler, G., & Das, S. (1998). An enhanced image of the Pamir-Hindu Kush seismic zone from relocated earthquake hypocentres. *Geophysical Journal International*, *134*(2), 573–595. https://doi.org/10.1046/j.1365-246X.1998.00582.x

Prieto, G. A., Beroza, G. C., Barrett, S. A., López, G. A., & Florez, M. (2012). Earthquake nests as natural laboratories for the study of intermediate-depth earthquake mechanics. *Tectonophysics*, *570–571*, 42–56. https://doi.org/10.1016/j.tecto.2012.07.019

Reigber, C., Michel, G. W., Galas, R., Angermann, D., Klotz, J., Chen, J. Y., et al. (2001). New space geodetic constraints on the distribution of deformation in Central Asia. *Earth and Planetary Science Letters*, *191*(1–2), 157–165. https://doi.org/10.1016/S0012-821X(01)00414-9

Reilinger, R., Mcclusky, S., Vernant, P., Lawrence, S., Ergintav, S., Cakmak, R., et al. (2006). GPS constraints on continental deformation in the Africa-Arabia-Eurasia continental collision zone and implications for the dynamics of plate interactions. *Journal of Geophysical Research*, *111*, B05411. https://doi.org/10.1029/2005JB004051

Roecker, S. W. (1982). Velocity structure of the Pamir-Hindu Kush Region: Possible evidence of subducted crust. *Journal of Geophysical Research*, *87*(B2), 945–959. https://doi.org/10.1029/JB087iB02p00945

Roecker, S. W., Soboleva, O. V., Nersesov, I. L., Lukk, A. A., Hatzfeld, D., Chatelain, J.-L., & Molnar, P. (1980). Seismicity and fault plane solutions of intermediate depth earthquakes in the Pamir-Hindu Kush region. *Journal of Geophysical Research*, *85*(B3), 1358–1364. https://doi.org/10.1029/JB085iB03p01358

Sangha, S., Peltzer, G., Zhang, A., Meng, L., Liang, C., Lundgren, P., & Fielding, E. (2017). Fault geometry of 2015, Mw7. 2 Murghab, Tajikistan earthquake controls rupture propagation: Insights from InSAR and seismological data. *Earth and Planetary Science Letters*, *462*, 132–141. https://doi.org/10.1016/j.epsl.2017.01.018

Schneider, F. M., Yuan, X., Schurr, B., Mechie, J., Sippl, C., Haberland, C., et al. (2013). Seismic imaging of subducting continental lower crust beneath the Pamir. *Earth and Planetary Science Letters*, *375*, 101–112. https://doi.org/10.1016/j.epsl.2013.05.015

Schurr, B., Ratschbacher, L., Sippl, C., Gloaguen, R., Yuan, X., & Mechie, J. (2014). Seismotectonics of the Pamir. *Tectonics*, *33*, 1501–1518. https://doi.org/10.1002/2014TC003576

Sippl, C., Schurr, B., Tympel, J., Angiboust, S., Mechie, J., Yuan, X., et al. (2013). Deep burial of Asian continental crust beneath the Pamir imaged with local earthquake tomography. *Earth and Planetary Science Letters*, *384*, 165–177. https://doi.org/10.1016/j.epsl.2013.10.01.3

Sippl, C., Schurr, B., Yuan, X., Mechie, J., Schneider, F. M., Gadoev, M., et al. (2013). Geometry of the Pamir-Hindu Kush intermediate-depth earthquake zone from local seismic data. *Journal of Geophysical Research: Solid Earth*, *118*, 1438–1457. https://doi.org/10.1002/jgrb.50128

Sobel, E. R., Chen, J., Schoenbohm, L. M., Thiede, R., Stockli, D. F., Sudo, M., & Strecker, M. R. (2013). Oceanic-style subduction controls late Cenozoic deformation of the Northern Pamir orogen. *Earth and Planetary Science Letters*, *363*, 204–218. https://doi.org/10.1016/j.epsl.2012.12.009

Sobel, E. R., Schoenbohm, L. M., Chen, J., Thiede, R., Stockli, D. F., Sudo, M., & Strecker, M. R. (2011). Late Miocene-Pliocene deceleration of dextral slip between Pamir and Tarim: Implications for Pamir orogenesis. *Earth and Planetary Science Letters*, *304*(3–4), 369–378. https://doi.org/10.1016/j.epsl.2011.02.012

Stein, S., & Stein, C. A. (1996). Thermo-mechanical evolution of oceanic lithosphere: Implications for the subduction process and deep earthquakes. In *Subduction: Top to bottom*, *Geophysical Monograph Series* (Vol. 96, pp. 1–17). Washington, DC: American Geophysical Union.

Strecker, M. R., Frisch, W., Hamburger, M. W., Ratschbacher, L., Semiletkin, S., Zamoruyev, A., & Sturchio, N. (1995). Quaternary deformation in the Eastern Pamirs, Tadzhikistan and Kyrgyzstan. *Tectonics*, *14*(5), 1061–1079. https://doi.org/10.1029/95TC00927

Szeliga, W., Bilham, R., Kakar, D. M., & Lodi, S. H. (2012). Interseismic strain accumulation along the western boundary of the Indian subcontinent. *Journal of Geophysical Research*, *117*, B08404. https://doi.org/10.1029/2011JB008822

Trifonov, V. G. (1978). Late Quaternary tectonic movements of western and central Asia. *Geological Society of America Bulletin*, *89*(7), 1059–1072. https://doi.org/10.1130/0016-7606(1978)89<1059:LQTMOW>2.0.CO;2

Trifonov, V. G. (1983). *Late Quaternary tectogenesis* [in Russian] (224 pp.). Nauka, Moscow.

Turcotte, D. L., Haxby, W. F., & Ockendon, J. R. (1977). Lithospheric instabilities, 1, 63–69. In M. Talwani, W. C. Pitman, & W. M. Ewing (Eds.), *Island arcs, deep sea trenches, and back-arc basins* (pp. 1, 57–61). Washington, DC: American Geophysical Union. https://doi.org/10.1029/ME001p0063

Vinnik, L. P., & Lukk, A. A. (1973). Velocity inhomogeneities in the upper mantle of Central Asia [in Russian]. *Doklady Akademii Nauk SSSR*, *213*(3), 580–583.

Vinnik, L. P., & Lukk, A. A. (1974). Lateral inhomogeneities in the upper mantle under the Pamir-Hindu Kush [in Russian]. *Izvestiya of the Academy of Sciences, USSR Physics Solid Earth*, *1*, 9–22.

Wessel, P., Smith, W. H. F., Scharroo, R., Luis, J., & Wobbe, F. (2013). Generic mapping tools: Improved version released. *Eos, Transactions American Geophysical Union*, *94*(45), 409–410. https://doi.org/10.1002/2013EO450001

Zhan, Z., & Kanamori, H. (2016). Recurring large deep earthquakes in Hindu Kush driven by a sinking slab. *Geophysical Research Letters*, *43*, 7433–7441. https://doi.org/10.1002/2016GL069603

Zhou, Y., He, J., Oimahmadov, I., Gadoev, M., Pan, Z., Wang, W., et al. (2016). Present-day crustal motion around the Pamir Plateau from GPS measurements. *Gondwana Research*, *35*, 144–154. https://doi.org/10.1016/j.gr.2016.03.011

Zubovich, A., Schöne, T., Metzger, S., Mosienko, O., Mukhamediev, S., Sharshebaev, A., & Zech, C. (2016). Tectonic interaction between the Pamir and Tien Shan observed by GPS. *Tectonics*, *35*, 283–292. https://doi.org/10.1002/2015TC004055

Zubovich, A. V., Wang, X. Q., Scherba, Y. G., Schelochkov, G. G., Reilinger, R., Reigber, C., Mosienko, O. I., et al. (2010). GPS velocity field for the Tien Shan and surrounding regions. *Tectonics*, *29*, TC6014. https://doi.org/10.1029/2010TC002772